Smart Photothermal-Triggered Bilayer Phase Transition in AuNPs-Liposomes to Release Drug

ARTICLE *in* LANGMUIR · JANUARY 2013

Impact Factor: 4.46 · DOI: 10.1021/la304692h · Source: PubMed

3 AUTHORS, INCLUDING:

Xueqin An
East China University of Science and Technology
141 PUBLICATIONS **1,328** CITATIONS

Langmuir

Article

pubs.acs.org/Langmuir

Smart Photothermal-Triggered Bilayer Phase Transition in AuNPs–Liposomes to Release Drug

Xueqin An,*[,†,‡] Fan Zhan,[‡] and Yinyan Zhu[‡]

[†]School of Chemistry and Molecular Engineering, East China University of Science and Technology, Shanghai, 200237, China

[‡]School of Chemistry and Materials Science, Nanjing Normal University, Nanjing, Jiangsu, 210097, China

ABSTRACT: Novel thermosensitive liposomes with embedded Au nanoparticles (AuNPs) in the liposome bilayer were prepared by a combination method of film build and supercritical CO_2 incubation. These AuNPs–liposomes possess AuNPs that are embedded in the bilayer and a drug that is encapsulated in the central aqueous compartment. The AuNPs in the liposomes can strongly absorb light energy and efficiently convert the absorbed energy to heat. The localized heat induces a phase transition in the liposome bilayer and releases the drug. The drug release from the AuNPs–liposomes can be controlled by the irradiation time and AuNPs concentration in the AuNPs–liposomes at room temperature, where the AuNPs function as a nanoswitch for triggering drug release both spatially and temporally. The results suggest that drug release from the AuNPs–liposomes is due to a photothermic effect that induces phase transition of the liposomes rather than destruction of the liposome bilayer.

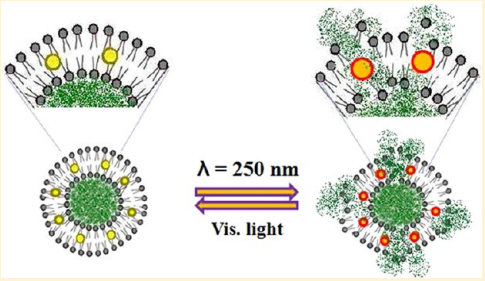

1. INTRODUCTION

Biomimetic liposomes are self-assembling structures in a lipid dispersion in water and a useful tool for drug delivery as a container for the storage, transfer, and controllable release of agents.[1] Liposomes have been recognized as drug nanocarriers for decades, but their clinical applications are often limited by uncontrolled release or poor availability of the encapsulated drug and stability in vivo in humans. A major challenge for drug delivery is controlled release both spatially and temporally.[2−4] For this reason, many of the current methods to enhance temporal or spatial control of drug release focus on incorporating components to achieve thermal,[5] pH,[6,7] photothermal,[8] magnetic,[9−12] or enzymatic[13] triggered release. Thermosensitive liposomes with a lower critical solution temperature (LCST) are a common drug carrier that function by thermostimulated drug release. The LCST is the phase transition temperature for gel to liquid crystalline transition in the liposomes. Traditional thermosensitive liposomes have been designed that release their drug loads when heated to the LCST. Consequently, the LCST is a very important parameter for the release of drug from thermosensitive liposomes. Nevertheless, it is difficult to control the LCST of liposomes using traditional methods because LCST can be affected by the type of drug, additive, medium pH value, etc.[14] For common photosensitive liposomes, triggered release of drugs occurs by using high-power laser light[15] or by destroying liposome stability using UV–visible light,[16] but these methods may damage cell membranes through the use of high power and long irradiation time.[15,16] Controlled drug release and the mechanism employed to release the drug are hence of utmost importance and remain a challenging problem. Research has focused on controlled drug release both spatially and temporally.[17]

Gold nanoparticles (AuNPs) have attracted much attention recently because of their interesting shape-dependent and size-dependent physical and chemical properties, which are very different from those of bulk gold and gold atoms.[18,19] Especially, AuNPs can strongly absorb light and efficiently convert the absorbed light to heat on a picosecond time scale.[20−23] The heat from the photothermal effect will dissipate into the bilayer surroundings in the liposomes, and the rise in temperature will cause the liposome phase transition of gel to liquid crystalline and result in drug release.[8,24] For those reasons, the optical and photothermal properties of AuNPs can be used for clinical application.[25] AuNPs show great promise as light-controlled molecular release systems.[26,27] Recent research work revealed that the calcein release temperature in liposomes with gold nanoparticles was decreased about 2 °C because of the addition of AuNPs,[28] membrane fluidity of the liposomes was increased above the LCST, ,[29] and AuNPs can absorb UV or near-IR light to induce drug release from liposomes.[2,8,17]

Berberine is an alkaloid found in medicinal plants, which has a wide range of biochemical and pharmacologic effects, including antitumor activity, but it can cause cacoethic actions in intravenous injection.[30] It has been reported to exhibit inhibitory and antitumor effects on esophageal cancer cells (ECCs)[31] and liver cancer cell line HepG2.[28] In this work, berberine was used as a model drug to study the functions of AuNPs–liposomes.

Received: November 26, 2012
Revised: December 29, 2012
Published: January 4, 2013

   dx.doi.org/10.1021/la304692h | *Langmuir* 2013, 29, 1061−1068

In this report, hydrophobic AuNPs (size about 5 nm) were prepared in AOT/heptane/water microemulsion. A thermosensitive liposome with AuNPs embedded in the bilayer and with berberine in the central aqueous compartment was synthesized by the combination method of film build and supercritical CO_2 incubation ($scCO_2$). The morphology and size of the AuNPs−liposomes were determined by transmission electron microscopy (TEM) and a light scattering method, and the property and function of the liposomes were studied. The aim of this study is to show that a drug encapsulated in AuNPs−liposomes is released by light irradiation at short times at room temperature, where the AuNPs are a nanoswitch for controlled drug release both spatially and temporally (Scheme 1), and to prove that the drug release from the liposomes is due to the photothermic effects that induce phase transition of the liposomes rather than destruction of the liposome structure.

Scheme 1. Drug Release from the AuNPs−Liposomes by Light Irradiation at Room Temperature

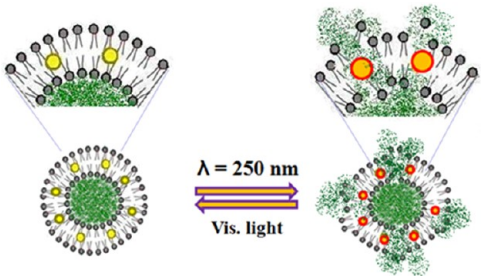

2. EXPERIMENTAL SECTION

2.1. Materials. Egg yolk lecithin (A.R.) and cholesterol (A.R.) were purchased from China Medicine Shanghai Chemistry Corporation. Berberine (≥98%) was purchased from the Northeast Medicine Factory. Sodium dioctyl sulfosuccinate (AOT, ≥96%) was purchased from Alfa Aesar. Chloroauric acid ($(HAucl_4{\cdot}3H_2O)$, ≥99.9%) was purchased from Sinopharm Chemical Reagent Beijing Co., Ltd. Chloroform, ethanol, hydrazine, and other chemical reagents were A.R grade.

2.2. Preparation of the Hydrophobic Gold Nanoparticles (AuNPs) in a Microemulsion. Two microemulsions (0.1 M $HAuCl_4$ solution/AOT/heptane and 2.0 M N_2H_4 solution/AOT/heptane) were prepared. The two microemulsions were mixed by vigorous magnetic stirring, the mixture turned red after 5 min, and AuNPs were synthesized. Then the AuNPs were separated with a high-speed centrifuge and were washed twice with aqueous ethanol solution (20%) and pure ethanol to remove byproducts. Finally, the AuNPs were dissolved in chloroform, and a stable, dark-brown AuNP chloroform solution was obtained. AuNPs with various sizes were synthesized by controlling the molar ratio (ω) of water to AOT from 5 to 15 in the water-in-oil microemulsion of water/AOT/isooctane.[5,32]

2.3. Preparation of AuNPs−Liposomes. Egg yolk lecithin and cholesterol (molar ratio of lecithin to cholesterol: 3/1) were dissolved in chloroform/methanol (2/1) solution. The lecithin−cholesterol solution was mixed with the AuNP chloroform solution, the organic solvent of the mixture was removed by rotary evaporation, and a thin lipid film was formed on the sides of round-bottom flask at 37 °C under nitrogen atmosphere after about 2 h. The lipid film was dried to remove residual organic solvent by pumping about 90 min. To remove organic solvent completely, the lipid film was pumped for 6 h and kept overnight in a vacuum tank. The dry film containing AuNPs and aqueous berberine solution (1 mg/mL) were transferred into a high-pressure cell and incubated by introducing CO_2 at 45 °C and a pressure of 16 MPa for 30 min. After incubation, the CO_2 was released very slowly, and a limpid, transparent AuNPs−liposome solution was obtained.

2.4. Size and Morphology of AuNPs and AuNPs−Liposomes. Size and morphology were determined by TEM for AuNPs and AuNPs−liposomes. TEM measurements were performed with a Hitachi H7650 instrument operated at 120 kV accelerating voltage. The samples were prepared by pipetting a drop of nanoparticle chloroform solution on carbon-coated copper grids and drying in air. The size of AuNPs−liposomes was also determined by a light scattering method (BI-200SM, Brookhaven Instruments).

2.5. Stability of AuNPs−Liposomes. The stability of the AuNPs−liposomes was estimated by measuring the transmission of the liposome solution using a UV−vis spectrophotometer (Aglient UV-8453) at various times. The stability constant (K_E) of the liposomes was calculated by the following equation:

$$K_E = (A_o - A_i)/A_o \quad (1)$$

A_0 and A_i are the transmissions of the AuNPs−liposomes prepared freshly and the AuNPs−liposomes stored for one month (277.2 K) at a wavelength of 500 nm and at 298.15 K, respectively. K_E is the stability constant; the smaller the value of K_E, the more stable the liposomes.

2.6. FT-IR Spectroscopy of AuNPs. FT-IR spectroscopy of heptane, AOT heptane solution, and AuNPs synthesized in AOT microemulsion were obtained using a Tensor 27 FT-IR spectrophotometer (Bruker Co.). Before testing the samples, an IR spectrum of the sample cuvette was taken as a background reference which was subtracted from the sample's spectrum.

2.7. Lower Critical Solution Temperature (LCST) of AuNPs−Liposomes. The lower critical solution temperature (LCST) of AuNPs−liposomes was determined by differential scanning calorimetry (Pyris Diamond DSC) to be about 41.7 °C.

2.8. Berberine Concentration Determined by Spectrophotometry. Absorbance ($A_{berberine}$) of berberine was measured at a wavelength of 345 nm using a UV−vis spectrophotometer (Agilent 8453E), and the berberine concentration can be derived by a standard curve of $C_{berberine}$ vs A. Berberine concentrations loaded in AuNPs−liposomes and released from the liposomes can be determined by measuring $A_{berberine}$ and deriving $C_{berberine}$ by using the standard curve.

2.9. Encapsulation Efficiency of Berberine in AuNPs−Liposomes. Before determination of berberine encapsulation efficiency in the AuNPs−liposomes, the dissociated berberine in the liposome solution was removed by dialysis, as described in the following steps. Berberine−AuNPs−liposomes solution was placed in the dialyzer (molecular weight: 8000−10000), the dialysis was performed by using water for 4 h, and the process was repeated many times until the dissociated berberine concentration approached zero in the solvent. The berberine concentration was measured with a UV−vis spectrophotometer to ensure the absence of berberine in the final dialysis process. All dialyzates were collected and transferred into a quantification vessel and filled with water to the scale of the vessel, and the absorbance (A) of berberine in the dialyzate was measured at λ_{345} with the UV spectrophotometer. The berberine concentration ($C_{berberine}$) in the dialyzate was determined using the standard curve of A vs $C_{berberine}$. The encapsulation efficiency ($Q_{encapsulation}$) of the berberine in AuNPs−liposomes can be calculated as follows:

$$Q_{encapsulation} = \frac{C_{total} - C_{dissociated}}{C_{total}} \times 100\% \quad (2)$$

C_{total} is the total berberine concentration, and $C_{dissociated}$ is the dissociated berberine concentration in the solution.

2.10. Heat-Induced Berberine Release from Liposomes. Liposomes with berberine were prepared by the $scCO_2$ method, and dissociated berberine in the liposomes was removed by dialysis. Berberine in the liposomes was released at various temperatures, and the berberine release rates from liposomes are calculated as follows:

dx.doi.org/10.1021/la304692h | Langmuir 2013, 29, 1061−1068

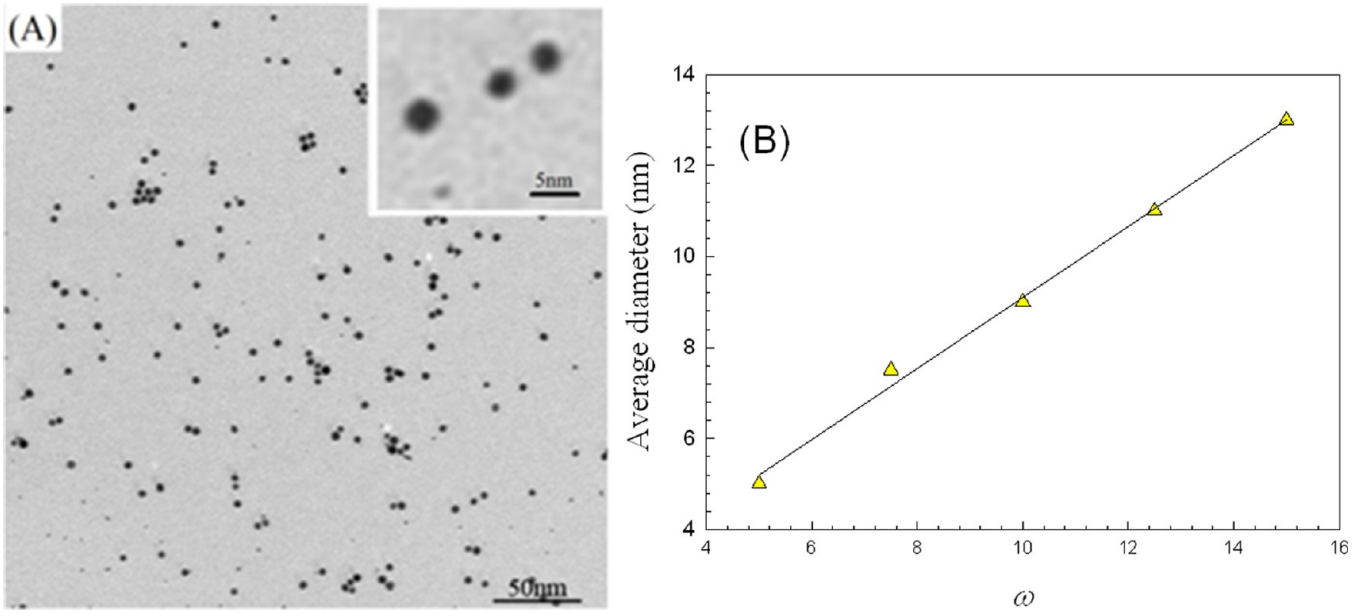

Figure 1. (A) TEM images of AuNPs synthesized in AOT microemulsion. (B) Variation of AuNP average diameter as a function of ω..

$$Q_{release} = \frac{C_{release}}{C_{total} - C_{dissociated}} \times 100\% = \frac{C_{release}}{C_{encapsulation}} \times 100\% \quad (3)$$

$C_{release}$ is the berberine concentration released from the liposomes. $C_{encapsulation}$ is $C_{total} - C_{dissociated}$ as the berberine encapsulation concentration in liposomes. Variation of berberine released from liposomes as a function of temperature and a release curve at various temperatures were obtained.

2.11. UV Light-Induced Berberine Release from AuNPs–Liposomes. For the continuous irradiation experiment, the berberine release experiments were performed by continuous irradiation with 250 nm wavelength UV light (60 W) or visible light (60 W) for 30 min at room temperature, respectively. After each irradiation, the berberine concentration released from the liposomes was determined using spectrophotometry, and the berberine release rates were calculated using eq 3. The relationship between various irradiation times and berberine concentration released from the liposomes was obtained.

To prove that the drug release from the AuNPs–liposomes was photothermally triggered, the berberine release experiments were performed by alternating irradiation with UV and visible light. The AuNPs–liposomes were irradiated by alternating UV light for 2.5 min and visible light for 5 min at room temperature, and this process was repeated many times. After the irradiation, berberine concentrations released from the liposomes were determined using spectrophotometry, and the berberine release rates were calculated using eq 3. The release curves were obtained at various irradiation times.

3. RESULTS AND DISCUSSION

3.1. Size and Morphology of AuNPs. Gold nanoparticles (AuNPs) are very different from those of bulk gold and gold atoms because of their interesting shape-dependent and size-dependent physical and chemical properties.[19,33] AuNPs can strongly absorb light and efficiently convert optical energy into localized heat, producing a selective photothermal effect.[23,31] In this work, hydrophobic AuNPs were prepared in AOT microemulsion, and the morphologies and the sizes of the AuNPs were observed with TEM, and all of the AuNPs were spherical and relatively monodispersed at 4–5 nm diameter (see insert in Figure 1A). The size of AuNPs was controlled by varying the molar ratio (ω) of water to AOT from 5 to 15 in a water-in-oil microemulsion. The average diameter of AuNPs increases with ω, and the results are shown in Figure 1B. Due to the existence of specific interactions between AuNPs and the AOT polar headgroup (Scheme 2A), AuNPs were entrapped in the core of the AOT microemulsion and surrounded by the hydrophobic tails of AOT as shown in Scheme 2B, which make the AuNPs hydrophobic and stable.[34]

Scheme 2. (A) AOT Structure. (B) AuNPs Surrounded by AOT

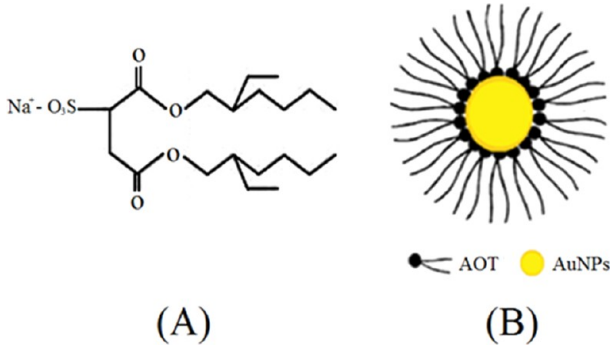

FT-IR was used as a nonperturbing technique to analyze possible changes in the structure of gold assemblies. These changes can be used to extract information about various physicochemical processes taking place in the systems.[35] To explain the hydrophobic properties of AuNPs, analyze the interaction of AOT with the AuNPs, and explore the effect of AOT on AuNP stability, various infrared spectra were obtained and are shown in Figure 2. Figure 2A,C shows IR spectra for heptane and AuNPs synthesized in AOT microemulsion, respectively. Compared with the IR spectrum of AOT in heptane solution (Figure 2B), the broadened resonance peak of the sulfonic group, which results from the synergistic effect of the absorption of the sulfonic group and C–O–C, is weakened and red-shifts from 1218 cm^{-1} to 1240 cm^{-1}. Another resonance peak of the sulfonic group, at 1046 cm^{-1}, is also an obvious aggrandizement. However, the resonance peak of

dx.doi.org/10.1021/la304692h | Langmuir 2013, 29, 1061–1068

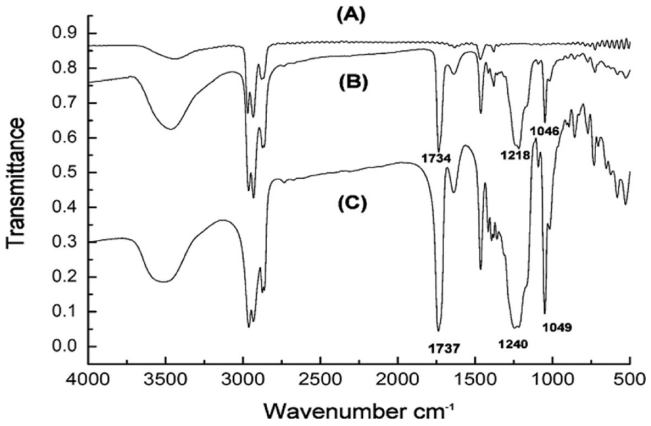

Figure 2. Infrared spectra at wavenumbers between 4000 and 500 cm^{-1}. (A) Heptane; (B) AOT in heptane solution; (C) AuNPs in AOT microemulsion.

the carbonyl (at 1734 cm^{-1}) changes little in absorption strength and wavenumber migration. The changes in the spectrum indicate that the coordination between the sulfonic group and AuNPs is the main action, and the action between the carbonyl and AuNPs is less important. The hydrophilic sulfonic groups of AOT reacted with the AuNP surface, and the hydrophobic carbonyl groups of AOT encircled the AuNPs, resulting in a protection layer on the surface of the AuNPs, as shown in Scheme 2B. As a result, AuNPs encircled by AOT are hydrophobic and will easily move into the phospholipid bilayer of the liposomes.

3.2. Lower Critical Solution Temperature of Liposomes and Controlled Release of Drugs. The lower critical solution temperature (LCST) of liposomes is the phase transition temperature of gel to liquid crystalline in the liposomes, which can be used to control release of drugs.[8,36−39] To prove that the liposomes are thermosensitive and that the drug is released by a thermoinduced phase transition, liposome-encapsulated berberine without AuNPs was prepared by the combination method of film build and $scCO_2$ incubation. The LCST was determined by differential scanning calorimetry (DSC) and is shown in Figure 3. The results reveal that the liposomes were thermosensitive and the LCST was about 41.7 °C. The liposome-encapsulated berberine was released at various temperatures, and the results demonstrate that berberine encapsulated in the liposomes almost could not be released when the temperature was below 41 °C but was released quickly when the temperature was raised to 42 °C as shown in Figure 4. This means that the liposomes were thermosensitive and that berberine encapsulated in the liposomes was released by thermoinduced phase transition above the LCST.

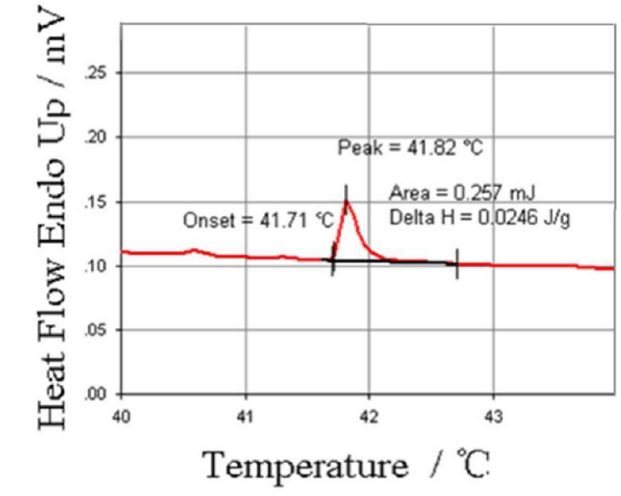

Figure 3. Lower critical solution temperature (LCST) of liposomes (DSC).

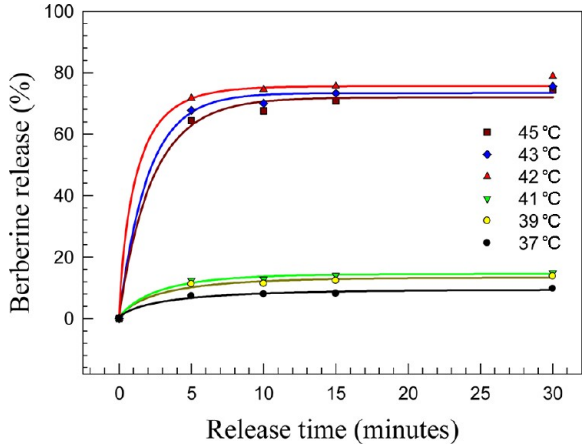

Figure 4. Berberine was released from thermosensitive liposomes at various temperatures.

3.3. Size, Morphology, and Properties of AuNPs−Liposomes. AuNPs−liposomes were prepared by the $scCO_2$ incubation method, which allows us to control the size and stability of the liposomes by adjusting preparation pressure and to adjust release ability by changing the molar proportion of the phospholipid to AuNP. AuNPs−liposomes with various AuNP concentrations were synthesized in the $scCO_2$ fluid, hydrophobic AuNPs (4−5 nm) were loaded into the liposome bilayer,[8] and berberine as a model drug was encapsulated in the central aqueous compartment of the AuNPs−liposomes (Scheme 3). The morphologies and sizes of the AuNPs−liposomes were observed with transmission electron microscopy (TEM) as shown in Figure 5. The liposomes were surrounded by AuNPs as spherical doughnut shapes, and the sizes of AuNPs−liposomes were about 150−200 nm. The amount of AuNPs surrounding the liposomes increased with AuNP concentration (C_{AuNPs}) (Figure 5, panels 2−6). From these images, it is supported that AuNPs could be entrapped in the hydrophobic bilayer of liposomes when C_{AuNPs} was below 11.5 μM, and dissociated AuNPs were detected clearly in the medium when C_{AuNPs} was above 22.5 μM (Figure 5, panel 6).

Scheme 3. Berberine Encapsulated in AuNPs−Liposomes

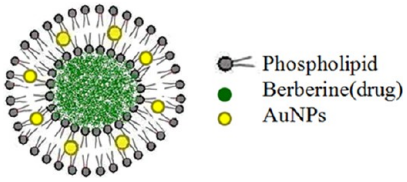

The encapsulation efficiency of berberine in the AuNPs−liposomes was determined by measuring absorbance of total berberine in the liposomes and dissociated berberine,

dx.doi.org/10.1021/la304692h | Langmuir 2013, 29, 1061−1068

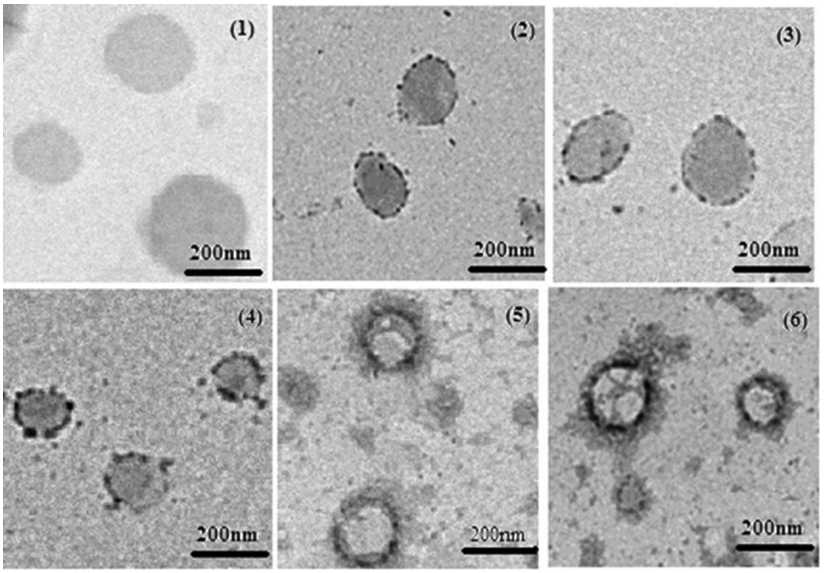

Figure 5. TEM images for AuNPs–liposomes with various C_{AuNPs} values: (1) 0 μM; (2) 4.5 μM; (3) 6.5 μM; (4) 9.0 μM; (5) 11.5 μM; (6) 22.5 μM.

converting to berberine concentration, and calculating $Q_{encapsulation}$ using eq 2. The berberine encapsulation efficiency in the AuNPs–liposomes with various C_{AuNPs}values was studied, and the results are shown in Figure 6. The

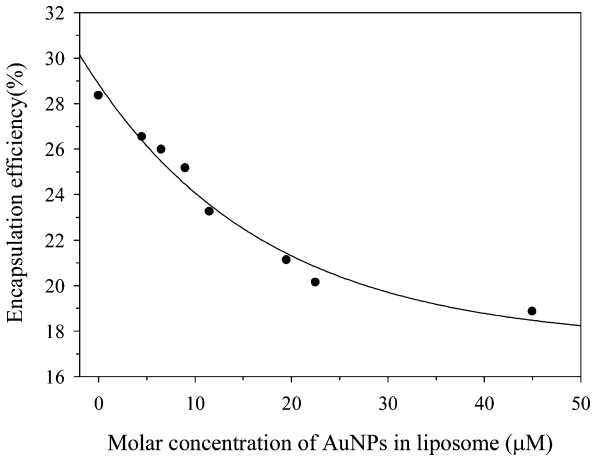

Figure 6. Effect of AuNP concentration on the berberine encapsulation efficiency.

encapsulation efficiency of AuNPs increases with a decrease in C_{AuNPs} for the AuNPs–liposomes possibly because the bilayer microstructure of liposomes was changed from the addition of AuNPs and because some space in the liposomes was occupied by the added AuNPs. Therefore, AuNPs not only move into the bilayer of the liposomes but also embed in other spaces of the liposomes, which leads to decreased berberine encapsulation. Considering the effect of AuNP addition on drug encapsulation efficiency, the best AuNP concentration for encapsulation was determined as 9.0 μM.

The stability constant (K_E) is an important parameter to represent the apparent stability of liposomes. It can be used to probe the liposome stability changes with time in aqueous solution; the smaller the value of K_E, the greater the stability. The values of K_E were obtained by measuring the changes in transmission of the aqueous liposome solutions at different times and calculating with eq 1. The variation in K_E as a function of C_{AuNPs} is shown in Figure 7. The values of K_E were

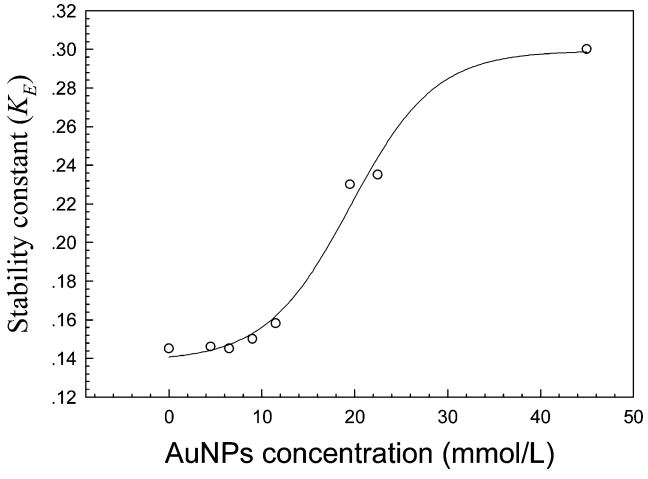

Figure 7. Stability constant (K_E) of AuNPs–liposomes at various C_{AuNPs} values for one month.

almost constant at C_{AuNPs} less than 11.5 μM, because AuNPs easily enter into the liposome bilayer at lower C_{AuNPs}. At a AuNP concentration (C_{AuNPs}) range of 11.5–45 μM, K_E increases with C_{AuNPs}, possibly because the AuNPs not only occupied the bilayer of liposomes but also embedded in the other spaces of the liposomes. Therefore, the microstructure of the liposomes was changed and the stability was decreased.

3.4. Light-Induced Berberine Release from AuNPs–Liposomes. We know that AuNPs can absorb light energy, which can be converted into localized heat, producing a selective photothermal effect. To explore the effect of different wavelengths of light on drug release, berberine release from AuNPs–liposomes was induced by UV (wavelength of 250 nm) and visible light irradiation at various irradiation times and at room temperature, respectively. The concentration of berberine released by UV irradiation was much higher than that by visible light irradiation as shown in Figure 8. This means

dx.doi.org/10.1021/la304692h | *Langmuir* 2013, 29, 1061–1068

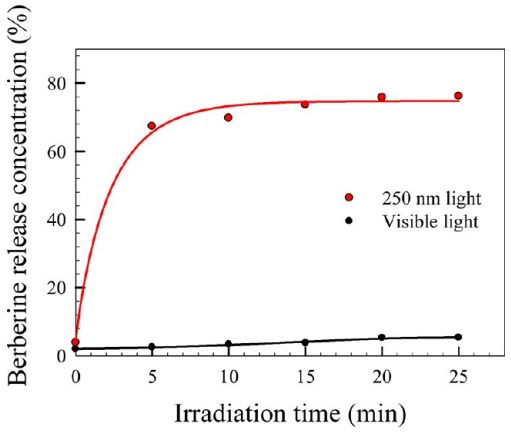

Figure 8. Berberine released from AuNPs–liposomes with different irradiation times at room temperature.

that AuNPs selectively absorbed UV light energy (wavelength of 250 nm) and suggests that the UV light (250 nm) triggered a phase transition of the AuNPs–liposomes at room temperature. AuNPs loaded in the liposome bilayer can strongly absorb UV light at room temperature and efficiently convert optical energy into localized heat, producing a selective photothermal effect, inducing phase transition of the liposomes, and releasing berberine from the liposomes.

To further demonstrate that AuNPs in the liposomes act as a nano-photothermal switch for drug release, the berberine encapsulated in liposomes at various C_{AuNPs} values was released at room temperature by a light-triggered mechanism. The berberine in liposomes without AuNPs almost cannot be released (Figure 9A, black line), and the release of berberine in AuNPs–liposomes increases with the C_{AuNPs} of AuNPs–liposomes, as shown in Figure 9A, colored lines. Berberine in AuNPs–liposomes was released very quickly at room temperature by UV irradiation, and over 50% of the berberine was released from the AuNPs–liposomes (C_{AuNPs} = 9.0 μM) in only 5 min (yellow line in Figure 9A). This drug release rate is much faster than that observed in previous research work.[36,37,40,41]

The effect of C_{AuNPs} on the drug release from the liposomes was studied, and the variation of berberine released from AuNPs–liposomes as a function of C_{AuNPs} after 20 min is shown in Figure 9B. The amount of berberine released from the liposomes increases linearly with C_{AuNPs} at C_{AuNPs} less than 11.5 μM, and it increases slightly with C_{AuNPs} at C_{AuNPs} higher than 11.5 μM. This means that most AuNPs could be entrapped in the hydrophobic bilayer of the liposomes at low C_{AuNPs} (>11.5 μM) because the AuNPs in the bilayer easily absorb light energy, produce the photothermal effect, and induce the phase transition that causes drug release. The berberine release rate increases slightly with C_{AuNPs} at higher C_{AuNPs} because the AuNPs not only move into the liposome bilayer but also into other spaces of the liposomes at high C_{AuNPs} (>11.5 μM) and AuNPs outside the bilayer cannot provide enough energy to heat the liposome bilayer to cause phase transition. The results are consistent with that obtained from TEM (Figure 5), and the optimal C_{AuNPs} in the liposomes is about 11.5 μM for this AuNPs–liposomes system. The

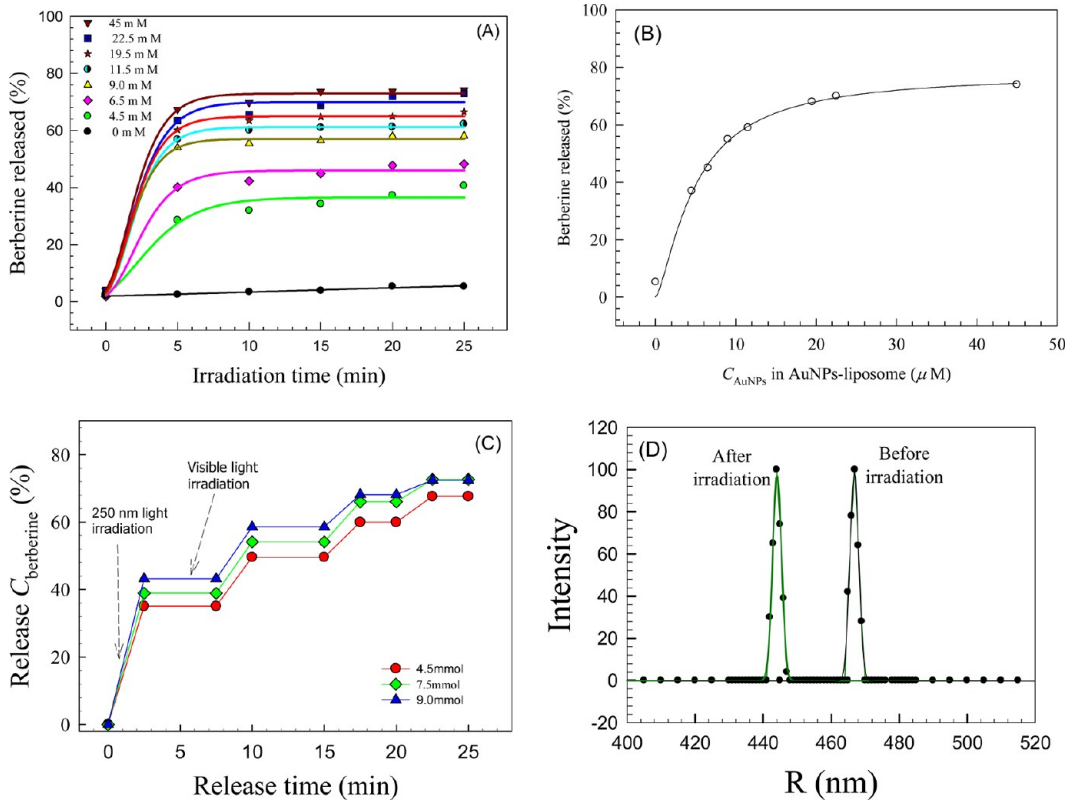

Figure 9. (A) Berberine released from AuNPs–liposomes at various C_{AuNPs} values by 250 nm UV light irradiation at room temperature. (B) Variation in berberine released from AuNPs–liposomes as a function of C_{AuNPs} after irradiation for 20 min. (C) Repetitious release from AuNPs–liposomes at various C_{AgFNPs} values by commutative irradiation with UV light and visible light. (D) Size of liposomes before and after release as determined by a light scattering method.

dx.doi.org/10.1021/la304692h | *Langmuir* 2013, 29, 1061–1068

results also reveal that the AuNPs in the liposomes are a switch for drug release, and the berberine amount released and the release rate can be controlled by the AuNP concentration in the liposomes and by irradiation time.

To further prove that the photothermic effect induces phase transition in the liposomes rather than destroys the bilayer of the liposomes, repetitious release of berberine encapsulated in AuNPs–liposomes at different C_{AuNPs} values was undertaken by commutative UV (2.5 min) and visible (5 min) light irradiation. The amounts of berberine released from the liposomes were measured, and the variation in berberine released from the AuNPs–liposomes as a function of release time is shown in Figure 9C. An important feature of the plots in Figure 9C is that berberine can be released repetitively from AuNPs–liposomes, and the amount of released berberine increases with C_{AuNPs} in the liposomes for the first release process, and the amount of released berberine decreases gently with increasing times. The results of berberine release by commutative irradiation suggest that berberine release from the liposomes is due to the selective photothermic effects inducing phase transition of the liposomes rather than destruction of the liposome structure. The results also reveal that the AuNPs in the liposomes function as a switch for drug release, and the switch can be controlled as "on-off" by UV irradiation. This means that the amount released from the liposomes can be controlled by UV irradiation time and intensity.

The sizes of liposomes before and after drug release were measured by the light scattering method, and the results are shown in Figure 9D. The size of particles before release is larger than that after release, and the difference is about 22 nm. The results also prove that the effect of the UV irradiation is to trigger phase transition and release drug rather than to destroy the bilayer of the liposomes.

4. CONCLUSION

Hydrophobic AuNPs were prepared in AOT/heptane/water microemulsion. Thermosensitive AuNPs–liposomes were prepared by the combination method of film build and supercritical CO_2 incubation. The morphology and size of the AuNPs–liposomes were determined by TEM and a light scattering method, and their properties and function were studied. The results reveal that the AuNPs–liposomes can strongly absorb certain wavelengths of light and efficiently convert it into localized heat, inducing phase transition and releasing drug. The drug can be released both by the heat generated by the photothermal effect from external UV irradiation and by the temperature increase of the local environmental media. The AuNPs in the liposomes act as a nanoswitch for drug release, and controlled berberine release both spatially and temporally can be carried out by adjustment of the AuNP concentration in the liposomes and irradiation time. The results also prove that berberine release from the liposomes is due to the photothermic effects that induce phase transition of the liposomes rather than destruction of the liposome structure.

AUTHOR INFORMATION

Corresponding Author

*Phone: 86-21-64250804; fax: 86-21-64250804; e-mail: anxueqin@ecust.edu.cn.

Notes

The authors declare no competing financial interest.

ACKNOWLEDGMENTS

This work is financially supported by the National Nature Science Foundation of China (21273073 and 21073063), the Nature Science Keystone Foundation of Shanghai (08jc1408100), and the Fundamental Research Funds for the Central Universities, China (No. WK0913002).

REFERENCES

(1) Chandrawati, R.; Caruso, F. Biomimetic liposome- and polymersome-based multicompartmentalized assemblies. *Langmuir* **2012**, *28*, 13798–13807.

(2) Volodkin, D. V.; Skirtach, A. G.; Mohwald, H. Remote near-IR Light activation of a hyaluronic acid/poly(L-lysine) multilayered film and film-entrapped microcapsules. *Angew. Chem., Int. Ed.* **2009**, *48*, 1807–1809.

(3) Kim, D. K.; Dobson, J. Nanomedicine for targeted drug delivery. *J. Mater. Chem.* **2009**, *19*, 6294–6307.

(4) Hsu, L.; Weder, C.; Rowan, S. J. Stimuli-responsive, mechanically-adaptive polymer nanocomposites. *J. Mater. Chem.* **2011**, *21*, 2812–2822.

(5) Hong, J. S.; Stavis, S. M.; Lacerda, S. H. D.; Locascio, L. E.; Raghavan, S. R.; Gaitan, M. Microfluidic-directed self-assembly of liposome–hydrogel hybrid nanoparticles. *Langmuir* **2010**, *26*, 11581–11588.

(6) Zhou, W.; An, X.; Wang, J.; Shen, W.; Chen, Z. Characteristics, Phase behavior and control release for copolymer–liposome with both pH and temperature sensitivities. *Colloids Surf., A* **2012**, *395*, 225–232.

(7) Yang, X.; Wang, Y.; Huang, X.; Ma, Y.; Huang, Y.; Yang, R.; Duan, H.; Chen, Y. Multi-functionalized graphene oxide based anticancer drug-carrier with dual-targeting function and pH-sensitivity. *J. Mater. Chem.* **2011**, *21*, 3448–3454.

(8) An, X.; Zhang, F.; Zhu, Y.; Shen, W. Photoinduced drug release from thermosensitive AuNPs-liposome using a AuNPs-switch. *Chem. Commun.* **2010**, *46*, 7202–7204.

(9) Qiu, D.; An, X. Microstructure study of liposomes decorated by hydrophobic magnetic nanoparticles. *Chem. Phys. Lipids* **2012**, *165*, 563–570.

(10) Hoare, T.; Santamaria, J.; Goya, G. F.; Irusta, S.; Lin, D.; Lau, S.; Padera, R.; Langer, R.; Kohane, D. S. A magnetically triggered composite membrane for on-demand drug delivery. *Nano Lett.* **2009**, *9*, 3651–3657.

(11) Meledandri, C. J.; Ninjbadgar, T.; Brougham, D. F. Size-controlled magnetoliposomes with tunable magnetic resonance relaxation enhancements. *J. Mater. Chem.* **2011**, *21*, 214–222.

(12) Benyettou, F.; Chebbi, I.; Motte, L.; Seksek, O. Magneto-liposome for alendronate delivery. *J. Mater. Chem.* **2011**, *21*, 4813–4821.

(13) Vemula, P. K.; Cruikshank, G. A.; Karp, J. M.; John, G. Self-assembled prodrugs: An enzymatically triggered drug-delivery platform. *Biomaterials* **2009**, *30*, 383–393.

(14) Gibson, M. I.; Paripovic, D.; Klok, H. A. Size-dependent LCST transitions of polymer-coated gold nanoparticles: cooperative aggregation and surface assembly. *Adv. Mater.* **2010**, *22*, 4721–4725.

(15) Ebrahim, S.; Peyman, G. A.; Lee, P. J. Applications of liposomes in ophthalmology. *Surv. Ophthalmol.* **2005**, *50*, 167–182.

(16) Mueller, A.; Bondurant, B.; O'Brien, D. F. Visible-light-stimulated destabilization of PEG–liposomes. *Macromolecules* **2000**, *33*, 4799–4804.

(17) Wu, G. H.; Milkhailovsky, A.; Khant, H. A.; Fu, C.; Chiu, W.; Zasadzinski, J. A. Remotely triggered liposome release by near-infrared light absorption via hollow gold nanoshells. *J. Am. Chem. Soc.* **2008**, *130*, 8175–8177.

(18) Burda, C.; Chen, X. B.; Narayanan, R.; El-Sayed, M. A. Chemistry and properties of nanocrystals of different shapes. *Chem. Rev.* **2005**, *105*, 1025–1102.

(19) Shaw, C. P.; Fernig, D. G.; Lévy, R. Gold nanoparticles as advanced building blocks for nanoscale self-assembled systems. *J. Mater. Chem.* **2011**, *21*, 12181–12187.

(20) Au, L.; Zheng, D. S.; Zhou, F.; Li, Z. Y.; Li, X. D.; Xia, Y. N. A quantitative study on the photothermal effect of immuno gold nanocages targeted to breast cancer cells. *ACS Nano* **2008**, *2*, 1645−1652.
(21) Liu, G. L.; Kim, J.; Lu, Y.; Lee, L. P. Optofluidic control using photothermal nanoparticles. *Nat. Mater.* **2006**, *5*, 27−32.
(22) Yavuz, M. S.; Cheng, Y. Y.; Chen, J. Y.; Cobley, C. M.; Zhang, Q.; Rycenga, M.; Xie, J. W.; Kim, C. K.; Song, H.; Schwartz, A. G.; Wang, L. H. V.; Xia, Y. N. Gold nanocages covered by smart polymers for controlled release with near-infrared light. *Nat. Mater.* **2009**, *8*, 935−939.
(23) Chen, H. J.; Shao, L.; Ming, T. A.; Sun, Z. H.; Zhao, C. M.; Yang, B. C.; Wang, J. F. Understanding the photothermal conversion efficiency of gold nanocrystals. *Small* **2010**, *6*, 2272−2280.
(24) Pentak, D.; Kowski, W. W. S.; Sulkowska, A. Calorimetric and EPR studies of the thermotropic phase behavior of phospholipid membranes. *J. Therm. Anal. Calorim.* **2008**, *93*, 471−477.
(25) Boisselier, E.; Astruc, D. Gold nanoparticles in nanomedicine: preparations, imaging, diagnostics, therapies and toxicity. *Chem. Soc. Rev.* **2009**, *38*, 1759−1782.
(26) Huang, J.; Jackson, K. S.; Murphy, C. J. Polyelectrolyte wrapping layers control rates of photothermal molecular release from gold nanorods. *Nano Lett.* **2012**, *12*, 2982−2987.
(27) Dave, N.; Liu, J. Protection and promotion of UV radiation-induced liposome leakage via DNA-directed assembly with gold nanoparticles. *Adv. Mater.* **2011**, *23*, 3182−3209.
(28) Paasonen, L.; Laaksonen, T.; Johans, C.; Yliperttula, M.; Kontturi, K.; Urth, A. Gold nanoparticles enable selective light-induced contents release from liposomes. *J. Controlled Release* **2007**, *122*, 86−93.
(29) Lee, S. M.; Park, H.; Yoo, K. H. Synergistic cancer therapeutic effects of locally delivered drug and heat using multifunctional nanoparticles. *Adv. Mater.* **2010**, *22*, 4049−4053.
(30) Shan, W.; Huang, L.; Zhou, Q.; Meng, F.; Li, X. Synthesis, biological evaluation of 9-N-substituted berberine derivatives as multifunctional agents of antioxidant, inhibitors of acetylcholinesterase, butyrylcholinesterase and amyloid-β aggregation. *Eur. J. Med. Chem.* **2011**, *46*, 5885−5893.
(31) Skrabalak, S. E.; Chen, J. Y.; Sun, Y. G.; Lu, X. M.; Au, L.; Cobley, C. M.; Xia, Y. N. Gold nanocages: synthesis, properties, and applications. *Acc. Chem. Res.* **2008**, *41*, 1587−1595.
(32) Ranjan, R.; Vaidya, S.; Thaplyal, P.; Qamar, M.; Ahmed, J.; Ganguli, A. K. Controlling the size, morphology, and aspect ratio of nanostructures using reverse micelles: a case study of copper oxalate monohydrate. *Langmuir* **2009**, *25*, 6469−6475.
(33) Balasubramanian, S. K.; Yang, L. M.; Yung, L. Y. L.; Ong, C. N.; Ong, W. Y.; Yu, L. E. Characterization, purification, and stability of gold nanoparticles. *Biomaterials* **2010**, *31*, 9023−9030.
(34) Zhang, F.; Qi, W.; An, X.; Zhu, Y. Controlled synthesis of gold nanoparticles and optical property in reverse microemulsions. *Rare Metal Mater. Eng.* **2011**, *40*, 2055−2059.
(35) Severcan, F.; Gorgulu, G.; Gorgulu, S. T.; Guray, T. Rapid monitoring of diabetes-induced lipid peroxidation by Fourier transform infrared spectroscopy: evidence from rat liver microsomal membranes. *Anal. Biochem.* **2005**, *339*, 36−40.
(36) Oddo, L.; Masci, G.; Meo, C.; Di; Capitani, D.; Mannina, L.; Lamanna, R.; De Santis, S.; Alhaique, F.; Coviello, T.; Matricardi, P. Novel thermosensitive calcium alginate microspheres: physico-chemical characterization and delivery properties. *Acta Biomater.* **2010**, *6*, 3657−3664.
(37) Kono, K.; Ozawa, T.; Yoshida, T.; Ozaki, F.; Ishizaka, Y.; Maruyama, K.; Kojima, C.; Harada, A.; Aoshima, S. Highly temperature-sensitive liposomes based on a thermosensitive block copolymer for tumor-specific chemotherapy. *Biomaterials* **2010**, *31*, 7096−7105.
(38) Quan, C.; Wei, H.; Shi, Y.; Li, Z.; Cheng, S.; Zhang, X.; Zhuo, R. Ag nanoparticle-embedded one-dimensional β-CD/PVP composite nanofibers prepared via electrospinning for use in antibacterial material. *Colloid Polym. Sci.* **2011**, *289*, 667−675.
(39) Kono, K.; Nakashima, S.; Kokuryo, D.; Aoki, I.; Shimomoto, H.; Aoshima, S.; Maruyama, K.; Yuba, E.; Kojima, C.; Harada, A.; Ishizaka, Y. Multi-functional liposomes having temperature-triggered release and magnetic resonance imaging for tumor-specific chemotherapy. *Biomaterials* **2011**, *32*, 1387−1395.
(40) Zhang, J. T.; Keller, T. F.; Bhat, R.; Garipcan, B.; Jandt, K. D. A novel two-level microstructured poly(N-isopropylacrylamide) hydrogel for controlled release. *Acta Biomater.* **2010**, *6*, 3890−3898.
(41) Aryal, S.; Grailer, J. J.; Pilla, S.; Steeber, D. A.; Gong, S. Q. Doxorubicin conjugated gold nanoparticles as water-soluble and pH-responsive anticancer drug nanocarriers. *J. Mater. Chem.* **2009**, *19*, 7879−7884.